

Evaluating and Mitigating Static Bias of Action Representations in the Background and the Foreground

Haoxin Li,¹ Yue Wu,² Yuan Liu,³ Hanwang Zhang,¹ Boyang Li¹

¹ Nanyang Technological University

² Damo Academy, Alibaba Group

³ Guangzhou University

haoxin003@e.ntu.edu.sg, matthew.wy@alibaba-inc.com, yuanliu@gzhu.edu.cn, hanwangzhang@ntu.edu.sg, boyang.li@ntu.edu.sg

Abstract

Deep neural networks for video action recognition easily learn to utilize shortcut static features, such as background and objects instead of motion features. This results in poor generalization to atypical videos such as soccer playing on concrete surfaces (instead of soccer fields). However, due to the rarity of out-of-distribution (OOD) data, quantitative evaluation of static bias remains a difficult task. In this paper, we synthesize new sets of benchmarks to evaluate static bias of action representations, including SCUB for static cues in the background, and SCUF for static cues in the foreground. Further, we propose a simple yet effective video data augmentation technique, StillMix, that automatically identifies bias-inducing video frames; unlike similar augmentation techniques, StillMix does not need to enumerate or precisely segment biased content. With extensive experiments, we quantitatively compare and analyze existing action recognition models on the created benchmarks to reveal their characteristics. We validate the effectiveness of StillMix and show that it improves TSM (Lin, Gan, and Han 2021) and Video Swin Transformer (Liu et al. 2021) by more than 10% of accuracy on SCUB for OOD action recognition.

Introduction

A major strength of deep neural networks (DNNs) is their ability to learn representations that transfer effectively to downstream tasks (Bengio, Courville, and Vincent 2013; Schmidhuber 2015). However, the quality of the learned representations degrades when the training data contain easy-to-learn shallow features that strongly correlate with the label. Often referred to as shortcut features, these features out-compete the hard-to-learn semantic features (Pezeshki et al. 2021; Hermann and Lampinen 2020), but do not generalize well to out-of-distribution data.

Shortcut feature learning is prevalent in video action recognition. DNNs can achieve decent accuracy relying on static objects (e.g., the soccer ball for the *soccer juggling* action), backgrounds (e.g., the golf course for *golf swinging*) and attributes of people (e.g., swimsuits for *swimming*). For example, with only static scene features, Li, Li, and Vasconcelos (2018) achieve an accuracy of 37% on HMDB51 (Kuehne et al. 2011), 18 times higher than chance level.

Though static features can lead to high accuracy when training and test data come from exactly the same distribution, their use may cause substantial performance drop un-

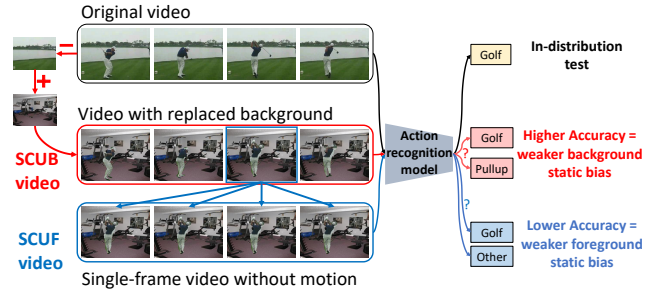


Figure 1: An illustration of benchmark construction. To quantify static cues in the background, we reserve the foreground actions and replace the backgrounds of original videos to synthesize videos with replaced background, named SCUB videos. To quantify static cues in the foreground, we randomly select one frame with replaced background and stack it into a single-frame video without motion, named SCUF videos.

der small distribution shifts, which are unavoidable in the real world. For example, constant changes in the design and style of swimsuits could break static features for the swimming action. In comparison, motion patterns of swimming are stable over time as they are built on human physiology. Thus, for effective action recognition in the wild, it is important to learn motion representations and suppress reliance on static cues.

A number of techniques have been proposed to mitigate scene bias (Choi et al. 2019; Wang et al. 2021; Zou et al. 2021; Ding et al. 2022; Zhang, Wang, and Ma 2021) and showed improved generalization on standard action datasets like UCF101 (Soomro, Zamir, and Shah 2012) and HMDB51 (Kuehne et al. 2011). However, as these test sets are largely identically distributed as the training sets, it is not immediately clear to what extent the performance improvements can be attributed to enhanced motion representations.

To facilitate quantitative evaluation and analysis of action representations, we create a new set of out-of-distribution (OOD) benchmarks. First, we utilize human annotations of UCF101 and HMDB51 datasets to extract the foregrounds of actions and replace the backgrounds with diverse natural and synthetic images. This procedure yields synthetic

test sets that can quantify representation bias toward static cues in the background (SCUB), where good motion features should perform well. Second, we create videos that repeat a single random frame from SCUB, producing test sets that can quantify representation bias toward static cues in the foreground (SCUF). As these videos disassociate the backgrounds from the action and contain no motion, their actions can be recognized by only static foreground features. Therefore, good performance on SCUF indicates stronger static bias. We illustrate the construction process in Figure 1.

With these benchmarks, we extensively evaluate several mainstream action recognition models and make the following observations. First, all mainstream models exhibit static bias. Second, performance on i.i.d. test data (*i.e.*, original UCF101 and HMDB51 test sets) is not a good indicator of robust action representations that generalize to OOD data. Third, debiasing methods, such as ActorCutMix (Zou et al. 2021) and FAME (Ding et al. 2022), demonstrate better resistance to background static cues than conventional training, but they remain vulnerable to foreground static bias.

An obstacle in suppressing foreground static features, such as swimsuits, is the difficulty to enumerate, locate, and separate them from the video. In contrast, ActorCutMix and FAME can locate and remove the background by segmenting humans and moving objects. Thus, it is desirable to learn to find bias-inducing content without the prior knowledge about their locations.

We propose a simple and effective video data augmentation technique StillMix, which identifies bias-inducing video frames using a reference network. After that, we mix videos with the bias-inducing still images but retain the original video labels in training a main network. Intuitively, this process randomly permutes labels for the bias-inducing still images, disrupting the association between the still images and action labels. This removes the need to explicitly extract the static bias with manually designed rules and facilitates the mitigation of static bias in the background and in the foreground. We empirically show that StillMix consistently boosts the performance of action recognition models and compares favorably with the other data augmentation techniques on both background and foreground bias. For example, it improves TSM and Video Swin Transformer by more than 10% of accuracy on SCUB and obtains around 4% of lower bias on SCUF.

The paper makes the following contributions:

- We create new benchmarks to quantitatively evaluate static bias of action representations in not only the background but also the foreground.
- We extensively compare mainstream action recognition models on the new benchmarks, revealing characteristics of these methods.
- We propose StillMix, a video data augmentation technique to mitigate background and foreground static bias.

Related Works

Action Recognition. 3D convolution or decomposed 3D convolutions (Ji et al. 2013; Tran et al. 2015; Carreira and Zisserman 2017; Varol, Laptev, and Schmid 2018; Tran

et al. 2018; Lin, Gan, and Han 2019) are popular choices for action recognition. Two-stream architectures employ two modalities, such as both RGB frames and optical flow (Simonyan and Zisserman 2014; Wang et al. 2018a), or videos with two different frame rates and resolutions (Feichtenhofer et al. 2019). Multi-scale temporal convolutions or feature fusion are designed for fine-grained actions with strong temporal structures (Zhou et al. 2018a; Hussein, Gavves, and Smeulders 2019; Li et al. 2020; Yang et al. 2020). Wang et al. (2018b) and Liu, Lee, and Jin (2019) employ self-attention to encode the global context. Recently, transformer networks are proposed to capture the long-range spatiotemporal dependencies (Arnab et al. 2021; Bertasius, Wang, and Torresani 2021; Liu et al. 2021). However, our understanding of the content of the representations learned by these models remains limited. In this paper, we create benchmarks to evaluate what features are captured by action models.

Evaluation of Static and Dynamic Information. Several works attempt to understand properties of spatiotemporal models with qualitative visualization (Feichtenhofer et al. 2020; Manttari et al. 2020). Ghodrati, Gavves, and Snoek (2018) designed proxy tasks to evaluate temporal asymmetry, continuity, and causality encoded by models. Hadji and Wildes (2018) introduced a dynamic texture dataset to evaluate appearance and dynamic information learning abilities of spatiotemporal models. Kowal et al. (2022) quantified the static and dynamic information in the learned representation using mutual information. However, they evaluated only static or dynamic information in the whole video, instead of static cues and motions in background and foreground specifically for human actions. In this paper, we create new benchmarks to evaluate static bias of action representations in background and foreground.

Static Bias in Videos. Current coarse-grained video action datasets contain bias toward static features, which easily induce the networks to learn static cues as shortcut features in action classification (Li, Li, and Vasconcelos 2018). Resound (Li, Li, and Vasconcelos 2018) and Repair (Li and Vasconcelos 2019) propose to downweight bias-inducing data points for reducing representation bias, but Wang et al. (2019) suggest merely weight adjustment is not sufficient. Wang and Hoai (2018) and Choi et al. (2019) aim to mitigate scene bias using conjugate samples, which are samples with similar contexts but different actions.

A few works are similar to the proposed StillMix technique. BE (Wang et al. 2021) mixes a frame from a video with all other frames in the same video. However, this still preserves the background scene information. ActorCutMix (Zou et al. 2021) and FAME (Ding et al. 2022) carefully cut the foreground, which may include the human actors or areas containing motion, from the background and replace the background with other images. SSVc (Zhang, Wang, and Ma 2021) and MCL (Li et al. 2021) focus the model to the spatiotemporal regions containing motion. However, it is difficult for these methods to separate static cues in the foreground from the motion information.

A particular advantage of StillMix is that it does not require an exhaustive list of possible types of bias as in Wang



Figure 2: Background images from different sources. (a) is an image from Place365. (b) is an image generated by VQGAN-CLIP from the query “A painting of a conference room in the style of surreal art”. (c) contains randomly generated sinusoidal stripes.

et al. (2019). Instead of manually designing procedures to separate the bias-inducing part of data, as in ActorCutMix, FAME, SSSVC and MCL, our method automatically identifies bias-inducing frames using a reference network. Consequently, StillMix can suppress static bias in both the background and the foreground of the videos, as shown in the experiments.

Benchmark Construction

To quantitatively evaluate foreground and background static bias of action representations, we create benchmarks based on UCF101 and HMDB51 datasets, as detailed below.

Foreground Annotations

To extract the foreground area of actions, we utilize available human annotations. For UCF101, we use human-annotated bounding boxes of people for 24 action classes provided by the Thumos challenge (Idrees et al. 2017). There are totally 910 videos in the test set having bounding box annotations. For HMDB51 dataset, we use human-annotated segmentation masks of people for 21 action classes from the JHMDB dataset (Jhuang et al. 2013). There are totally 256 videos in the test set having mask annotations.

Background Images

In order to synthesize diverse testing videos, we collect background images from different image sources. For each image source, we construct a background image pool from the following sources:

- All 328,500 images in the test set of Place365 (Zhou et al. 2018b).
- 2,000 images generated by VQGAN-CLIP (Crowson et al. 2022) from a random scene category of Place365 and a random artistic style.
- Randomly generated images with S-shaped stripes defined by sinusoid functions, which are parameterized by random colors, phases, frequencies, stripe widths, etc.

In Figure 2, we show three example background images from the three sources. For more details of the background image generation process, we refer readers to the appendix.

Test Video Synthesis

Testing for Background Static Cues. Given a video x with T frames $\{x_t\}_{t=1}^T$, we create a synthetic video \tilde{x} by combining the foreground action of x and a background image

Table 1: Statistics of the created benchmarks.

Video Source	# Original Videos	Background Source	# Synthetic Videos	# Domain Gap of SCUB	# Domain Gap of SCUF
UCF101	910	Place365	4,550	3.016 ± 0.111	3.033 ± 0.103
		VQGAN-CLIP	4,550	3.934 ± 0.112	4.002 ± 0.166
		Sinusoid	4,550	3.954 ± 0.068	3.957 ± 0.113
HMDB51	256	Place365	2,560	1.740 ± 0.037	1.737 ± 0.060
		VQGAN-CLIP	2,560	2.094 ± 0.081	2.121 ± 0.069
		Sinusoid	2,560	2.470 ± 0.027	2.475 ± 0.082

sampled from the background image pool.

$$\tilde{x}_t = m_t \odot x_t + (1 - m_t) \odot z_{bg}, \quad (1)$$

where m_t is the foreground mask obtained from the annotations. \odot denotes pixel-wise multiplication. z_{bg} is a background image sampled from the image pool. For each video with foreground annotations, we pair it with m randomly selected background images from each background image source to synthesize $3m$ videos. We set $m = 5$ for UCF101 and $m = 10$ for HMDB51 dataset, since HMDB51 has fewer human-annotated original videos and we would like to increase the diversity of the synthetic videos.

The generated videos retain the original action foreground, including the human actors and their motion, on new random backgrounds. They are designed to test for static cues from the background, and are named SCUB videos. A model invariant to static backgrounds should be able to obtain high classification accuracy on SCUB.

Testing for Foreground Static Cues. In addition, we create another set of videos to test the amount of foreground static bias in the learned representations. Examples of the foreground static cues include bicycle helmets for the cycling action and swimsuits for the swimming action — people can ride a bicycle without helmets or wear swimsuits when not swimming. As the SCUB videos contain most foreground elements in the original videos, they cannot distinguish whether models rely on foreground static cues in action recognition.

To this end, we create videos that contain only a single frame. Specifically, from each SCUB video, we randomly select one frame and repeat it temporally to create a video with zero motion. As these videos quantify the representation bias toward static cues in the foreground, which we name SCUF videos. In SCUF videos, the foreground static features are identical to the corresponding SCUB videos, but the motion information is totally removed. Therefore, a model invariant to foreground static features should obtain low classification accuracy on them.

We summarize the dataset statistics in Table 1. SCUB and SCUF have the same number of videos for each pair of video source and background source. As a proxy for background static bias, we also report the scene bias, explained in the next section.

Quality Assessment

We empirically verify that the SCUB dataset retains the motion features of the original videos but replaces background static features using the following two tests.

Human Assessment. To test if SCUB preserve the motion information sufficiently for action recognition, we carry out an experiment on Amazon Mechanical Turk (AMT) to verify if human workers can recognize the action in SCUB.

From the same original video, we randomly sampled one synthetic video and asked the AMT worker if the moving part in video shows the labeled action. The worker is given three options: yes, no, and can't tell. To detect random clicking, we created a number of control questions from 200 original videos and assigned both correct and incorrect labels. In addition, to prevent the workers from always answering yes to synthetic videos, we create a control group of 1,166 synthetic videos and assigned to them incorrect labels, so the workers ought to answer no. Workers who do not reach at least 80% accuracy on the control questions are rejected. The final answer for one video is obtained by majority voting of three different workers. Further details are in the appendix.

Collectively, the AMT workers were able to recognize the correct action in 96.15% of UCF101-SCUB and 86.33% of HMDB51-SCUB videos. We conclude that the synthetic videos preserve sufficient action information for humans to recognize.

Domain Gaps of the Static Features. To verify if SCUB replaces the background static features, we test if a classifier based on pure static features trained on the original UCF101 or HMDB51 can generalize to SCUB.

Using a variation of Choi et al. (2019), we define the domain gap G_{scene} as

$$G_{scene} = \ln[Acc(D_{old}, \Phi_{scene})/Acc(D_{SCUB}, \Phi_{scene})]. \quad (2)$$

Here Φ_{scene} is the average frame feature extracted from a ResNet-50 pretrained on Place365, a scene recognition dataset. Thus, the extracted feature captures static information, mostly from the background. We train a linear classifier on the original video dataset (UCF101 or HMDB51 respectively) and apply it to the original test set, obtaining accuracy $Acc(D_{old}, \Phi_{scene})$. After that, we apply the same classifier to SCUB, obtaining accuracy $Acc(D_{SCUB}, \Phi_{scene})$. A higher ratio indicates greater domain gap with respect to the static background features.

In Table 1, we show the means and standard deviations computed from three random repeats of video synthesis. We observe large domain gaps, up to $\exp(3.954) = 52$ -fold decrease in accuracy, which demonstrates the static features of SCUB videos differ substantially from the original videos and SCUB can successfully serve as out-of-distribution tests. Moreover, the low standard deviations show that the effects of random sampling are marginal. In later experiments, we use the dataset from one random seed.

The StillMix Technique

In order to learn action representations invariant to static cues, we propose a simple but effective video data augmentation algorithm, StillMix. Instead of using manually de-

signed rules to downweight or remove biased data from the training set, as in ActorCutMix or FAME, StillMix learns to identify still images that induce biased representation using a neural network. As a result, StillMix offers a flexible bias-suppressing technique that works for both the background and foreground.

We begin with some notations. We denote the i^{th} video in the training set as tensor $\mathbf{x}_i \in \mathbb{R}^{C \times T \times H \times W}$, where C , T , H and W are the number of channels, number of frames, height and width of the video, respectively. The associated ground-truth action label is y_i . The video \mathbf{x}_i contains a sequence of frames $\langle \mathbf{z}_{i,j} \rangle_{j=1}^T$, $\mathbf{z}_{i,j} \in \mathbb{R}^{C \times H \times W}$. The training set contains N training video samples and is written as $\{(\mathbf{x}_i, y_i)\}_{i=1}^N$. The goal of StillMix is to augment a given training sample (\mathbf{x}_i, y_i) into a transformed sample $(\tilde{\mathbf{x}}_i, \tilde{y}_i)$. The procedures of StillMix are illustrated in Figure 3 and introduced as follows.

Step 1: Training the Reference Network. In this paper, we identify bias-inducing still frames using a 2D convolutional network that predicts the action label from still frames of a video. As the still frames contain no motion, we expect the network to rely on static features to make the predictions.

Specifically, at every epoch we randomly extract a frame $\mathbf{z}_{i,j} \in \mathbb{R}^{C \times H \times W}$ from each video \mathbf{x}_i , and train the reference network $\mathcal{R}(\cdot)$ to predict the label y_i . The overall loss is

$$L_{ref} = \frac{1}{N} \sum_{i=1}^N \ell(\mathcal{R}(\mathbf{z}_{i,j}), y_i), \quad (3)$$

where $\ell(\cdot)$ can be any classification loss, such as the cross-entropy. After training, the reference network $\mathcal{R}(\cdot)$ encodes the correlations between static cues within the frames and the action classes.

Step 2: Identifying Biased Still Images. The output of reference network $\mathcal{R}(\mathbf{z}_{i,j})$ is a categorical distribution over action classes. We take the probability of the predicted class $p_{i,j} = \max_k P(y = k | \mathbf{z}_{i,j})$. A high $p_{i,j}$ indicates strong correlation between $\mathbf{z}_{i,j}$ and the action class, which means $\mathbf{z}_{i,j}$ can induce static representation bias. Therefore, we select frames with high $p_{i,j}$ to construct the bank of biased still images S :

$$S = \{\mathbf{z}_{i,j} | p_{i,j} > \tau\}, \quad (4)$$

where τ is a probability threshold. In practice, we perform another round of uniformly random selection to exactly control the size of the biased still image bank.

Step 3: Mixing Video and Biased Still Images. To break the strong correlation between the biased frame and the action class, we mix a still image identified above with videos from any action class. Specifically, given a video sample (\mathbf{x}_i, y_i) , we sample a biased still frame $\mathbf{z}^{\text{biased}}$ from the biased image bank S and tile it T times along the temporal dimension, yielding a static video with T identical frames. We denote this operation as $\text{Tile}(\mathbf{z}^{\text{biased}}, T)$. Then, the augmented video sample $\tilde{\mathbf{x}}_i$ is generated by the pixel-wise interpolation of \mathbf{x}_i and the static video. The augmented video label \tilde{y}_i is the same as the original action label y_i .

$$\tilde{\mathbf{x}}_i = \lambda \mathbf{x}_i + (1 - \lambda) \text{Tile}(\mathbf{z}^{\text{biased}}, T), \quad \tilde{y}_i = y_i, \quad (5)$$

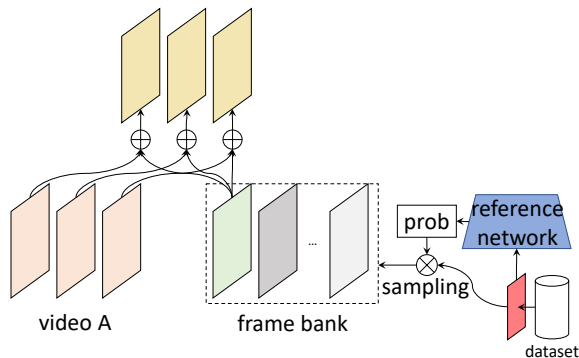


Figure 3: An illustration of StillMix. We extract frames with biased static using a reference network, which form a biased frame bank. We mix extracted frames from the frame bank with each frame in the original video (Video A) to generate an augmented video. \oplus denotes pixel-wise addition. \otimes denotes frame sampling.

where scalar λ is sampled from a Beta distribution $Beta(\alpha, \beta)$.

The rationale for keeping the video label unchanged after augmentation is that the static video contains no motion and should not contribute to the action label. This setting of StillMix can be intuitively understood as randomly permuting the labels of the static video, so that the network is forced to ignore the correlation between static cues and actions.

Training With Augmented Videos. We apply StillMix to each video with a predefined probability P_{aug} .

$$(\mathbf{x}_i^*, y_i^*) = \begin{cases} (\mathbf{x}_i, y_i) & a_i = 0 \\ (\tilde{\mathbf{x}}_i, \tilde{y}_i) & a_i = 1 \end{cases}, a_i \sim Ber(P_{\text{aug}}), \quad (6)$$

where a is a scalar sampled from a Bernoulli distribution $Ber(P_{\text{aug}})$. The samples $\{(\mathbf{x}_i^*, y_i^*)\}_{i=1}^N$ are used to train the final action recognition network $\mathcal{F}(\cdot)$ using the following loss function.

$$L = \frac{1}{N} \sum_{i=1}^N \ell(\mathcal{F}(\mathbf{x}_i^*), y_i^*), \quad (7)$$

where $\ell(\cdot)$ could be any classification loss.

Discussion. In principle, StillMix is similar to Nam et al. (2020) that use a reference network to identify bias-inducing data instances, but we identify bias-inducing components (frames) rather than whole data points (videos), which necessitates the mixing operation. In addition, we use a reference network (a 2D convolutional network) that differs from the main network (3D CNNs or transformer networks) to identify static bias from dynamic motions of human actions, whereas Nam et al. (2020) used identical networks.

Comparing to the background-replacing, foreground-preserving augmentations (e.g., ActorCutMix and FAME), StillMix mitigates static bias not only in the background but also in the foreground. Since ActorCutMix and FAME preserve the foreground, they do not remove static features

in the foreground. Instead, StillMix learns to identify static bias using a 2D network without explicitly defining where the static bias come from. In the next section, we show that StillMix learns action representations that are highly invariant to both foreground and background static features.

Experiments

In this section, we compare the performance of several mainstream action recognition models on the synthetic datasets and validate the effectiveness of StillMix.

Comparing Methods

Spatiotemporal Models. We compare three mainstream action recognition models on the synthetic datasets: (1) TSM (Lin, Gan, and Han 2021), a temporal shift module that learns spatiotemporal features with 2D CNN. (2) SlowFast (Feichtenhofer et al. 2019), a two-branch 3D CNN that learns spatiotemporal signals under two different frame rates. (3) Video Swin Transformer (Liu et al. 2021), an adapted Swin Transformer for video. We use the tiny version, Swin-T.

Debiasing Methods. We also compare two debiasing methods with publicly available models: (1) SDN (Choi et al. 2019), a model that minimizes scene information and maximizes human action information in learned representations using adversarial classifiers. (2) FAME (Ding et al. 2022), which carves out the foreground from the video for training to mitigate background bias.

Video Data Augmentation Baselines. We compare the debiasing performance of several video data augmentation methods by adapting them to supervised action recognition. (1) Mixup (Zhang et al. 2017) and VideoMix (Yun et al. 2020). (2) BE (Wang et al. 2021), ActorCutMix (Zou et al. 2021) and FAME (Ding et al. 2022). We use these three methods as data augmentation, which extracts the foreground and replaces the background as in the original papers. All the data augmentation techniques are applied stochastically. All hyperparameters are tuned on in-distribution validation data. For more details, please refer to the appendix.

Results and Analysis

We denote the original test data (i.e., videos in UCF101 and HMDB51 test sets) as in-distribution (IID) test data. In Table 2 and 3, we show the results of different action recognition models and debiasing methods on the IID test data and synthetic OOD tests. In Table 4 and 5, we compare the performance of different video data augmentation methods applied to Kinetics400-pretrained TSM and Swin-T. Note that higher accuracy on SCUB datasets is better (indicating low background static bias), while lower accuracy on SCUF datasets is better (indicating low foreground static bias).

Performance of different models. Comparing performance on IID and OOD tests, we observe that all the examined action recognition models perform much worse on SCUB tests than IID tests. Given that human workers can recognize these actions, the results indicate that these models in-

Table 2: Action recognition accuracy (%) of different methods on the UCF101, UCF101-SCUB and UCF101-SCUF datasets.

Method	Pretraining	UCF101	UCF101-SCUB (\uparrow)			UCF101-SCUF (\downarrow)		
			Place365	VQGAN-CLIP	Sinusoid	Place365	VQGAN-CLIP	Sinusoid
TSM	ImageNet	84.84	13.89	8.73	9.58	7.89	4.76	6.21
	Kinetics-400	94.62	26.79	22.66	27.36	5.63	4.12	2.89
SlowFast	ImageNet	80.82	15.14	11.37	8.91	6.63	3.90	3.45
	Kinetics-400	95.96	34.34	31.00	30.19	2.44	1.51	1.14
Swin-T	ImageNet	88.20	19.24	16.97	22.01	8.76	7.45	10.53
	Kinetics-400	96.21	37.63	34.37	54.94	3.48	3.02	10.82
SDN	Mini-Kinetics	84.17	10.31	7.82	8.59	1.85	1.47	1.69
FAME	Kinetics-400	88.60	18.79	19.06	15.80	1.25	1.21	1.27

Table 3: Action recognition accuracy (%) of different methods on the HMDB51, HMDB51-SCUB and HMDB51-SCUF datasets.

Method	Pretrain	HMDB51	HMDB51-SCUB (\uparrow)			HMDB51-SCUF (\downarrow)		
			Place365	VQGAN-CLIP	Sinusoid	Place365	VQGAN-CLIP	Sinusoid
TSM	ImageNet	47.56	19.39	16.99	8.49	11.78	11.12	6.41
	Kinetics-400	70.39	45.09	42.16	26.84	23.26	20.03	14.40
SlowFast	ImageNet	47.65	21.24	16.85	10.43	17.84	15.63	11.76
	Kinetics-400	76.25	47.36	48.23	35.00	23.26	23.14	18.78
Swin-T	ImageNet	53.62	23.45	19.39	18.24	18.25	14.80	15.94
	Kinetics-400	73.92	47.61	42.77	41.41	20.68	17.90	22.80
SDN	Mini-Kinetics	56.60	26.76	23.48	11.13	14.80	14.69	4.96
FAME	Kinetics-400	61.10	31.45	28.67	25.12	13.28	13.67	12.93

evitably capture static background features; when the backgrounds are replaced, performance drop ensues.

Comparing performance of different action recognition models, we observe that Swin-T obtains better accuracy on both IID test data and SCUB than TSM and SlowFast, while does not increase accuracy too much on SCUF. The results suggest that the transformer architecture learns more robust action features, though we refer readers to Pinto, Torr, and Dokania (2022) and Zhou et al. (2022) for further discussion. Still, the performance of Swin-T can be much improved by proper data augmentation methods, as shown in Table 4 and 5.

Effects of pretraining. Comparing ImageNet and Kinetics-400 as pretraining datasets, we observe that Kinetics-pretrained models improve the performance on both IID test and SCUB without too much performance sacrifice on SCUF. The results demonstrate that pretraining on large-scale video datasets is by itself an effective method to de-bias action representations. We hypothesize that the size of Kinetics-400 is so large that it contains reasonably balanced static cues. However, collecting, annotating, and training on large-scale datasets are still costly, while data augmentation methods could mitigate static bias even for Kinetics-pretrained models; the minimum improvement for Swin-

T is 10.88% on UCF101-SCUB-Sinusoid and 6.21% on HMDB51-SCUB-Place365.

Performance of video data augmentation methods. Comparing the performance of different augmentation methods in Table 4 and 5, we observe that all these data augmentation methods obtain similar accuracy on IID test data — the difference between the best and the worst accuracies is less than 1%. However, they show significantly different performance on SCUB and SCUF datasets. **This demonstrates that performance on IID test data alone is not a good indicator of robust and generalizable action representations.**

In particular, on Kinetics-pretrained models, the performances of Mixup, VideoMix and BE on OOD data are comparable to that without augmentation, indicating little debiasing effects. ActorCutMix and FAME demonstrate much improved invariance to background static bias on SCUB. Nevertheless, they decrease performance (increase accuracy) on SCUF, which suggests that their improved performance on SCUB is partially due to the use of foreground static features rather than motion features. The action features learned with ActorCutMix and FAME are still vulnerable to foreground static bias.

In contrast, StillMix boosts the performance not only on SCUB but also on SCUF videos. The significant improve-

Table 4: Action recognition accuracy (%) of augmentation methods on the UCF101, UCF101-SCUB and UCF101-SCUF datasets.

Model	Augmentation	UCF101	UCF101-SCUB (\uparrow)			UCF101-SCUF (\downarrow)		
			Place365	VQGAN-CLIP	Sinusoid	Place365	VQGAN-CLIP	Sinusoid
TSM	No	94.62	26.79	22.66	27.36	5.63	4.12	2.89
	Mixup	94.71	29.03	24.85	29.51	5.20	3.94	2.99
	VideoMix	94.50	32.76	29.99	31.89	6.73	5.63	4.94
	BE	94.49	27.25	22.99	27.52	6.07	4.42	3.36
	ActorCutMix	94.44	38.95	37.63	37.74	4.84	4.85	3.99
	FAME	93.72	36.80	37.76	32.61	4.63	4.10	2.28
	StillMix	94.30	37.40	33.85	40.30	0.97	0.81	0.60
Swin-T	No	96.21	37.63	34.37	54.94	3.48	3.02	10.82
	Mixup	96.17	39.82	40.89	57.79	2.88	3.28	11.62
	VideoMix	96.00	28.59	37.36	58.26	7.81	11.40	20.60
	BE	96.06	39.76	36.16	56.01	3.55	2.93	10.15
	ActorCutMix	95.87	51.02	55.28	69.53	8.00	8.43	19.32
	FAME	95.81	40.62	44.56	37.54	5.74	6.50	6.84
	StillMix	96.22	55.47	54.22	65.82	2.07	2.08	5.87

Table 5: Action recognition accuracy (%) of augmentation methods on the HMDB51, HMDB51-SCUB and HMDB51-SCUF datasets.

Model	Augmentation	HMDB51	HMDB51-SCUB (\uparrow)			HMDB51-SCUF (\downarrow)		
			Place365	VQGAN-CLIP	Sinusoid	Place365	VQGAN-CLIP	Sinusoid
TSM	No	70.39	45.09	42.16	26.84	23.26	20.03	14.40
	Mixup	72.00	46.25	44.07	28.96	22.60	19.92	14.71
	VideoMix	70.72	42.68	41.46	23.00	20.98	18.99	12.46
	BE	71.22	45.39	42.81	27.25	23.42	20.52	14.40
	ActorCutMix	70.52	45.81	42.32	27.08	23.29	22.43	15.12
	FAME	70.39	51.25	53.21	36.33	26.04	23.34	17.60
	StillMix	72.15	53.92	52.21	38.22	11.89	8.44	5.56
Swin-T	No	73.92	47.61	42.77	41.41	20.68	17.90	22.80
	Mixup	74.58	46.70	42.49	40.12	21.25	18.47	23.78
	VideoMix	73.31	41.33	38.18	38.67	19.64	18.82	22.85
	BE	74.31	47.36	42.94	40.39	20.91	17.55	21.41
	ActorCutMix	74.05	50.13	46.51	43.73	22.16	20.26	23.80
	FAME	73.79	54.71	53.67	45.81	27.10	27.26	26.40
	StillMix	75.25	53.82	52.49	50.02	13.04	13.13	14.97

ments on SCUF show that the improvements on SCUB of StillMix is quite different from ActorCutMix or FAME, *i.e.*, StillMix focuses on motion features instead of foreground static features. **This clearly demonstrates its ability to reduce static bias that is difficult to explicitly enumerate and manually extract**, *e.g.*, foreground static bias. For more experimental result, including Kinetics-pretrained SlowFast and ImageNet pretrained models, we refer readers to the appendix.

Performance of debiased pretraining. The debiasing methods SDN and FAME adopt debiased pretraining on large datasets and finetuning on UCF101 and HMDB51. SDN obtains comparable performance on IID test data and SCUB with ImageNet-pretrained models, but largely worse performance than Kinetics-pretrained models. FAME also lags behind Kinetics-pretrained models, although it is also pretrained on Kinetics-400. The results indicate that vanilla supervised pretraining is more effective than self-supervised

pretraining at mitigating static bias. Effective debiased self-supervised pretraining deserves further research attention.

Conclusion

To quantitatively evaluate static bias in action representations, we create two new sets of benchmarks, SCUB and SCUF, which can quantify static bias in background and foreground. Through extensive evaluation, we conclude that the performance on conventional IID test data alone is not a good indicator of robust and generalizable action representations. We also observe that existing debiasing methods like FAME remain vulnerable to foreground static bias despite their resistance to background static bias. To mitigate both background and foreground static bias, we propose a simple and effective video data augmentation technique, StillMix. Our experiments show that it consistently improves several action recognition models and exhibits superior mitigation of static bias over other video data augmentation methods.

References

- Arnab, A.; Deghani, M.; Heigold, G.; Sun, C.; Lučić, M.; and Schmid, C. 2021. Vivit: A video vision transformer. In *IEEE International Conference on Computer Vision*, 6836–6846.
- Bengio, Y.; Courville, A.; and Vincent, P. 2013. Representation Learning: A Review and New Perspectives. *IEEE Transactions on Pattern Analysis and Machine Intelligence*, 35(8): 1798–1828.
- Bertasius, G.; Wang, H.; and Torresani, L. 2021. Is Space-Time Attention All You Need for Video Understanding? *arXiv preprint arXiv:2102.05095*.
- Carreira, J.; and Zisserman, A. 2017. Quo Vadis, Action Recognition? A New Model and the Kinetics Dataset. In *IEEE Conference on Computer Vision and Pattern Recognition*, 4724–4733. IEEE.
- Choi, J.; Gao, C.; Messou, J. C.; and Huang, J.-B. 2019. Why Can't I Dance in the Mall? Learning to Mitigate Scene Bias in Action Recognition. In *Advances in Neural Information Processing Systems*.
- Crowson, K.; Biderman, S.; Kornis, D.; Stander, D.; Hallahan, E.; Castricato, L.; and Raff, E. 2022. Vqgan-clip: Open domain image generation and editing with natural language guidance. *arXiv preprint arXiv:2204.08583*.
- Ding, S.; Li, M.; Yang, T.; Qian, R.; Xu, H.; Chen, Q.; Wang, J.; and Xiong, H. 2022. Motion-Aware Contrastive Video Representation Learning via Foreground-Background Merging. In *Proceedings of the IEEE/CVF Conference on Computer Vision and Pattern Recognition (CVPR)*, 9716–9726.
- Feichtenhofer, C.; Fan, H.; Malik, J.; and He, K. 2019. Slow-fast networks for video recognition. In *IEEE international conference on computer vision*, 6202–6211.
- Feichtenhofer, C.; Pinz, A.; Wildes, R. P.; and Zisserman, A. 2020. Deep insights into convolutional networks for video recognition. *International Journal of Computer Vision*, 128(2): 420–437.
- Ghodrati, A.; Gavves, E.; and Snoek, C. G. 2018. Video time: Properties, encoders and evaluation. *arXiv preprint arXiv:1807.06980*.
- Hadji, I.; and Wildes, R. P. 2018. A new large scale dynamic texture dataset with application to convnet understanding. In *Proceedings of the European Conference on Computer Vision (ECCV)*, 320–335.
- Hermann, K.; and Lampinen, A. 2020. What shapes feature representations? exploring datasets, architectures, and training. *Advances in Neural Information Processing Systems*, 33: 9995–10006.
- Hussein, N.; Gavves, E.; and Smeulders, A. W. 2019. Timeception for Complex Action Recognition. In *IEEE Conference on Computer Vision and Pattern Recognition*, 254–263.
- Idrees, H.; Zamir, A. R.; Jiang, Y.; Gorban, A.; Laptev, I.; Sukthankar, R.; and Shah, M. 2017. The THUMOS challenge on action recognition for videos “in the wild”. *Computer Vision and Image Understanding*, 155: 1–23.
- Jhuang, H.; Gall, J.; Zuffi, S.; Schmid, C.; and Black, M. J. 2013. Towards understanding action recognition. In *IEEE international conference on computer vision*, 3192–3199.
- Ji, S.; Xu, W.; Yang, M.; and Yu, K. 2013. 3D Convolutional Neural Networks for Human Action Recognition. *IEEE Transactions on Pattern Analysis and Machine Intelligence*, 35(1): 221–231.
- Kowal, M.; Siam, M.; Islam, M. A.; Bruce, N. D.; Wildes, R. P.; and Derpanis, K. G. 2022. A Deeper Dive Into What Deep Spatiotemporal Networks Encode: Quantifying Static vs. Dynamic Information. In *Proceedings of the IEEE/CVF Conference on Computer Vision and Pattern Recognition*, 13999–14009.
- Kuehne, H.; Jhuang, H.; Garrote, E.; Poggio, T.; and Serre, T. 2011. HMDB: a large video database for human motion recognition. In *International conference on computer vision*, 2556–2563. IEEE.
- Li, R.; Zhang, Y.; Qiu, Z.; Yao, T.; Liu, D.; and Mei, T. 2021. Motion-Focused Contrastive Learning of Video Representations. In *IEEE International Conference on Computer Vision*, 2105–2114.
- Li, Y.; Ji, B.; Shi, X.; Zhang, J.; Kang, B.; and Wang, L. 2020. TEA: Temporal Excitation and Aggregation for Action Recognition. In *IEEE Conference on Computer Vision and Pattern Recognition*, 906–915.
- Li, Y.; Li, Y.; and Vasconcelos, N. 2018. Resound: Towards action recognition without representation bias. In *European Conference on Computer Vision*, 513–528.
- Li, Y.; and Vasconcelos, N. 2019. Repair: Removing representation bias by dataset resampling. In *Proceedings of the IEEE/CVF conference on computer vision and pattern recognition*, 9572–9581.
- Lin, J.; Gan, C.; and Han, S. 2019. TSM: Temporal Shift Module for Efficient Video Understanding. In *IEEE International Conference on Computer Vision*, 7083–7093.
- Lin, J.; Gan, C.; and Han, S. 2021. TSM: Temporal Shift Module for Efficient Video Understanding. In *IEEE International Conference on Computer Vision*, 7082–7092. IEEE.
- Liu, X.; Lee, J.-Y.; and Jin, H. 2019. Learning Video Representations From Correspondence Proposals. In *IEEE Conference on Computer Vision and Pattern Recognition*, 4273–4281.
- Liu, Z.; Ning, J.; Cao, Y.; Wei, Y.; Zhang, Z.; Lin, S.; and Hu, H. 2021. Video swin transformer. *arXiv preprint arXiv:2106.13230*.
- Manttari, J.; Broomé, S.; Folkesson, J.; and Kjellström, H. 2020. Interpreting video features: A comparison of 3D convolutional networks and convolutional LSTM networks. In *Proceedings of the Asian Conference on Computer Vision*.
- Nam, J.; Cha, H.; Ahn, S.; Lee, J.; and Shin, J. 2020. Learning from failure: De-biasing classifier from biased classifier. *Advances in Neural Information Processing Systems*, 33: 20673–20684.
- Pezeshki, M.; Kaba, O.; Bengio, Y.; Courville, A. C.; Precup, D.; and Lajoie, G. 2021. Gradient starvation: A learning proclivity in neural networks. *Advances in Neural Information Processing Systems*, 34: 1256–1272.

- Pinto, F.; Torr, P. H.; and Dokania, P. K. 2022. An Impartial Take to the CNN vs Transformer Robustness Contest. *arXiv preprint arXiv:2207.11347*.
- Schmidhuber, J. 2015. Deep learning in neural networks: An overview. *Neural Networks*, 61: 85–117.
- Simonyan, K.; and Zisserman, A. 2014. Two-Stream Convolutional Networks for Action Recognition in Videos. In *Advances in Neural Information Processing Systems*, 568–576.
- Soomro, K.; Zamir, A. R.; and Shah, M. 2012. UCF101: A dataset of 101 human actions classes from videos in the wild. *arXiv preprint arXiv:1212.0402*.
- Tran, D.; Bourdev, L.; Fergus, R.; Torresani, L.; and Paluri, M. 2015. Learning Spatiotemporal Features with 3D Convolutional Networks. In *IEEE International Conference on Computer Vision*, 4489–4497.
- Tran, D.; Wang, H.; Torresani, L.; Ray, J.; LeCun, Y.; and Paluri, M. 2018. A Closer Look at Spatiotemporal Convolutions for Action Recognition. In *IEEE Conference on Computer Vision and Pattern Recognition*, 6450–6459.
- Varol, G.; Laptev, I.; and Schmid, C. 2018. Long-Term Temporal Convolutions for Action Recognition. *IEEE Transactions on Pattern Analysis and Machine Intelligence*, 40(6): 1510–1517.
- Wang, J.; Gao, Y.; Li, K.; Lin, Y.; Ma, A. J.; Cheng, H.; Peng, P.; Huang, F.; Ji, R.; and Sun, X. 2021. Removing the background by adding the background: Towards background robust self-supervised video representation learning. In *IEEE Conference on Computer Vision and Pattern Recognition*, 11804–11813.
- Wang, L.; Xiong, Y.; Wang, Z.; Qiao, Y.; Lin, D.; Tang, X.; and Van Gool, L. 2018a. Temporal Segment Networks for Action Recognition in Videos. *IEEE Transactions on Pattern Analysis and Machine Intelligence*.
- Wang, T.; Zhao, J.; Yatskar, M.; Chang, K.-W.; and Ordonez, V. 2019. Balanced datasets are not enough: Estimating and mitigating gender bias in deep image representations. In *Proceedings of the IEEE/CVF International Conference on Computer Vision*, 5310–5319.
- Wang, X.; Girshick, R.; Gupta, A.; and He, K. 2018b. Non-local Neural Networks. In *IEEE Conference on Computer Vision and Pattern Recognition*, 7794–7803.
- Wang, Y.; and Hoai, M. 2018. Pulling actions out of context: Explicit separation for effective combination. In *IEEE Conference on Computer Vision and Pattern Recognition*, 7044–7053.
- Yang, C.; Xu, Y.; Shi, J.; Dai, B.; and Zhou, B. 2020. Temporal Pyramid Network for Action Recognition. In *IEEE Conference on Computer Vision and Pattern Recognition*, 588–597.
- Yun, S.; Oh, S. J.; Heo, B.; Han, D.; and Kim, J. 2020. Videomix: Rethinking data augmentation for video classification. *arXiv preprint arXiv:2012.03457*.
- Zhang, H.; Cisse, M.; Dauphin, Y. N.; and Lopez-Paz, D. 2017. mixup: Beyond empirical risk minimization. *arXiv preprint arXiv:1710.09412*.
- Zhang, M.; Wang, J.; and Ma, A. J. 2021. Suppressing Static Visual Cues via Normalizing Flows for Self-Supervised Video Representation Learning. *arXiv preprint arXiv:2112.03803*.
- Zhou, B.; Andonian, A.; Oliva, A.; and Torralba, A. 2018a. Temporal Relational Reasoning in Videos. In *European Conference on Computer Vision*, 831–846.
- Zhou, B.; Lapedriza, A.; Khosla, A.; Oliva, A.; and Torralba, A. 2018b. Places: A 10 Million Image Database for Scene Recognition. *IEEE Transactions on Pattern Analysis and Machine Intelligence*, 40(6): 1452–1464.
- Zhou, D.; Yu, Z.; Xie, E.; Xiao, C.; Anandkumar, A.; Feng, J.; and Alvarez, J. M. 2022. Understanding the robustness in vision transformers. In *International Conference on Machine Learning*, 27378–27394. PMLR.
- Zou, Y.; Choi, J.; Wang, Q.; and Huang, J.-B. 2021. Learning representational invariances for data-efficient action recognition. *arXiv preprint arXiv:2103.16565*.